

Chanamolu Swathi¹, Sangaraju Venkata Jagadeesh Chandra^{2*}, Yarravarapu Srinivasa Rao¹, Dodda Venkata Rama Koti Reddy¹

¹Department of Instrument Technology, AU College of Engineering, Andhra University, Visakhapatnam, Andhra Pradesh India, ²Department of Physics, GITAM School of Science, GITAM (Deemed to be) University, Rishikonda, Visakhapatnam-530045.

Scientific paper

ISSN 0351-9465, E-ISSN 2466-2585

<https://doi.org/10.62638/ZasMat1146>



Zastita Materijala 65 ()
(2024)

Influence of Nd dopant on the structural properties of barium zirconium titanate perovskite

ABSTRACT

Barium zirconium titanate (BZT) nanocomposite powder was prepared using the solid-state reaction method. To enhance the structural properties of BZT, neodymium (Nd) was doped at various concentration levels. The thermal stability of Nd-doped BZT was analyzed through a calcination process conducted at temperatures of 1150, 1200, 1250, 1300, and 1350 °C for 4 hours. The XRD spectra of the sample calcined at 1350 °C for 4 hours exhibited significant peaks compared to samples calcined at lower temperatures. The results indicated that the crystallographic properties of the sample improved with increasing Nd concentrations. FTIR spectra confirmed the presence of BZT and showed corresponding band shifts with the addition of Nd. As the Nd percentage in BZT increased, the broad band positions shifted to a higher wavenumber range, from [699–479] cm⁻¹ to [746–484] cm⁻¹. The crystallographic nature of TiO_x, ZrO_x, and Nd_xO_y compounds was confirmed by the vibrational band shifts towards a lower wavenumber range, from [746–484] cm⁻¹ to [735–480] cm⁻¹. Field emission scanning electron microscopy images revealed that Nd-doped BZT samples exhibited higher porosity compared to undoped BZT.

Keywords: Barium Zirconium Titanate, Neodymium, Ball milling, Crystallographic Structure, Surface morphology

1. INTRODUCTION

Multifunctional materials have potential applications in the field of not only in the area of microelectronics, but in diversified fields. In particular they have been widely used in piezoelectric transducers, dynamic random-access memories (DRAMs) electrical energy storage units & tunable microwave devices, green electronics, food packaging, sensors, tissue engineering applications, actuators, electromagnetic shielding, biomedical implants and other biomedical and electronic applications etc., [1-3], among various multifunctional materials, barium titanate (BaTiO₃) based compositions have been attracted great attention due to the compensated search for lead-free ferroelectric materials [4,5]. In particular, barium zirconium titanate (BZT) attracts the researchers over barium strontium titanate (BST) in the

fabrication of ceramic capacitors due to more chemical stability of Zr⁴⁺ when compare with Ti⁴⁺ [6,7].

In general, complex perovskites have the formula (AA¹) (BB¹) O₃ which contains both ordered/disordered structures, which are basically relaxor ferro electric materials [8,9]. Among various relaxor materials BZT grab attention of researchers for storage applications [10]. Various dopants have been added to BZT system to enhance the dielectric properties of the same [11]. Impurity doping is a major approach among many common ways to improve the material physical and electrical properties [3]. Addition of rare earth ions in BZT influences the dielectric properties, eventually the doped BZT ceramics have demonstrated potential applications not only for storage applications but also microwave applications [12]. By considering the potential applications of Barium based solid solutions for electronic devices and the role for various dopants, the objective of current research was initiated to study the structural and initial dielectric behavior of BZT system by doping with Neodymium (Nd). In this investigation we studied the effect of Nd percentage on structural,

Corresponding author: S.V. Jagadish Chandra

E-mail: jsangara@gitam.edu

Paper received: 12. 06. 2024.

Paper corrected: 19. 09. 2024.

Paper accepted: 10. 10. 2024.

compositional and surface morphological characteristics of BZT.

2. MATERIALS AND METHODS/ EXPERIMENTAL DETAILS

(Ba_{1-x}Nd_{2x/3}) (Zr_{0.3}Ti_{0.7}) O₃ (x = 0.05%, 0.1%, 0.15%, 0.2% and 0.25%) ceramics were prepared by the conventional high energy milling process with reagents commercial high purity powders (M/S Loba Company) of BaCO₃ (99.9%), ZrO₂ (99.9%), TiO₂ (99.9%) and Nd₂O₃ (99%pure, SRL) were weighed according to their stoichiometric ratio.

The Raw materials BaCO₃, ZrO₂, TiO₂ and Nd₂O₃ weighed according to their stoichiometric ratio with dopant Nd in order to prepare Sample-1 (Ba_{1-x} Nd_{2x/3}) (Zr_{0.3} Ti_{0.7}) O₃ (x = 0.05%) Sample-2 (Ba_{1-x} Nd_{2x/3}) (Zr_{0.3} Ti_{0.7}) O₃, (x = 0.1%) in a high energy planetary mono model ball mill, which contains station-1 & Station-2. Each station contains 250ml Tungsten carbide jar and tungsten balls (8mm Dia & 8grm weigh) by maintaining the ratio of powder to ball as 1:2.

With toluene C₇H₈ (M.W 92.14, 99% pure, SRL) as binding medium the samples are grinded for 12 hours continuously with a rotational speed of 200 rpm, with a short break of 10mins after every 30min of grinding to cool down the machine temperature. After 12 hours of grinding the wet sample was collected into ceramic crucible and Calcination of each sample was followed by heating in the air oven at 80 °C to dry the wet sample. The Same steps were repeated for other samples (x=0, 0.15%, 0.2% ,0.25%). All the dried samples were stored in the containers separately. Initially the Sample-1(X=0.05%) is weighed into 5 parts each of 2grms separately and collected into 99.7%Alumina Cylindrical Crucibles (C-100ml, OD-52mm, H-65mm) for optimizing temperatures to

perform the conventional calcination at 1150, 1200,1250,1300 and 1350 °C 4hrs in the box furnace of upto temperature 1500°C. All the calcinated samples were separately grinded manually in the in the Mortar and pestle continuously for 1hr to make into fine and smooth powder. For further more confirmation, perform the calcination process for different time intervals of 2 and 6 hour at the same temperature. Since the samples calcinated at 1350°C temperature for 4 hour confirmed the sharp peaks, the remaining samples (Nd=0, 0.1%, 0.15%,0.2%,0.25%) were also calcinated at 1350°C, 4hours.

Characterization techniques: X-ray powder diffraction (XRD) was used in the investigation of the crystallinity of the samples using a Bruker advanced D8 X-ray diffractometer. The pattern was recorded on "PANalytical EMPYREAN diffractometer" using Cu-K α radiation ($\lambda=1.5405 \text{ \AA}$ nm) in the 2θ range 20°–80°. Surface microstructure and grain size distribution of calcinated powders were examined by a Field Emission Scanning Electron Microscope, FE-SEM (Model-JEOL JSM-7600F, Japan) Fourier Transform Infrared spectra (FT-IR) were recorded for all using a Opus 7.0 software FT-IR spectrophotometer (Bruker Alfa-II).

3. RESULTS AND DISCUSSION

Crystallographic Structure

The comprehensive diffraction peaks of (Ba_{1-x}Nd_{2x/3}) (Zr_{0.3}Ti_{0.7})O₃ powder synthesized by high energy ball milling method were shown in Fig 1. The phase formation of BZT with Nd (Ba_{1-x}Nd_{2x/3}) (Zr_{0.3}Ti_{0.7}) O₃ at different temperatures illustrated below.

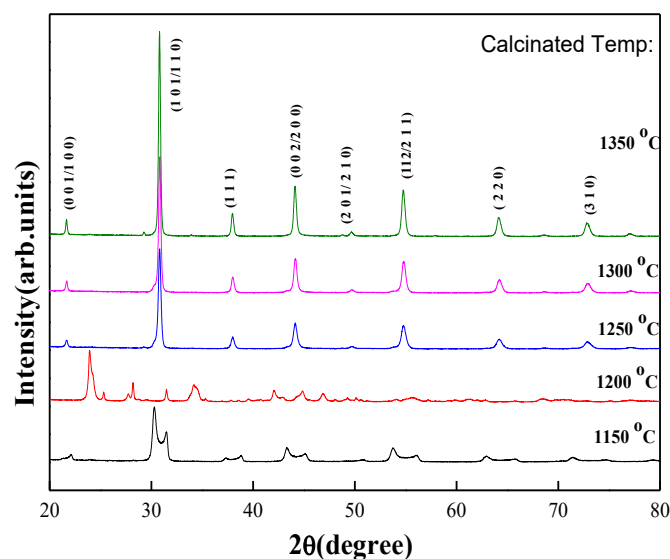


Figure 1. XRD profile of Nd doped BZT at various calcinated temperatures

On close observation of the XRD patterns listed from 1150 °C, 1200 °C, 1250 °C, 1300 °C and 1350 °C. The 1250 °C clearly confirmed the single-phase formation of $\text{Ba}_{1-x}\text{Nd}_{2x/3}\text{Zr}_{0.3}\text{Ti}_{0.7}\text{O}_3$. Any intermediate product formation was strictly not observed at and above 1250 °C. At 1150 °C, a trace amount of BaCO_3 was also observed in the XRD spectra in the 2θ range from 29 to 31°. This broad traces were disappeared entirely from the calcination temperature of 1250 °C and above. All the peaks observed at $2\theta = 21.65, 29.24, 31.2, 33.9, 37.9, 44.2, 54.6, 57.6, 64.1, 72.7$ are well matched with the standard patterns which are mostly corresponding to mixed phase of tetragonal

and cubic structures of 'Nd' doped BZT [13]. The significant peak (110).

Observed at the Bragg angle of 31.2° is attributed to the cubic structured 'Nd' doped BZT. The intensity of the peak observed at 31.2° has been increased significantly at the temperature of 1350 °C. Hence we considered the calcinated temperature of 1350 °C is optimized temperature to form single phase 'Nd' doped BZT. To know the effective optimized period of time to form the stable single phase 'Nd' doped BZT more accurately, performed the calcination process at three different time intervals and depict the crystallographic information by performing X-ray diffraction on these three samples in Fig. 2.

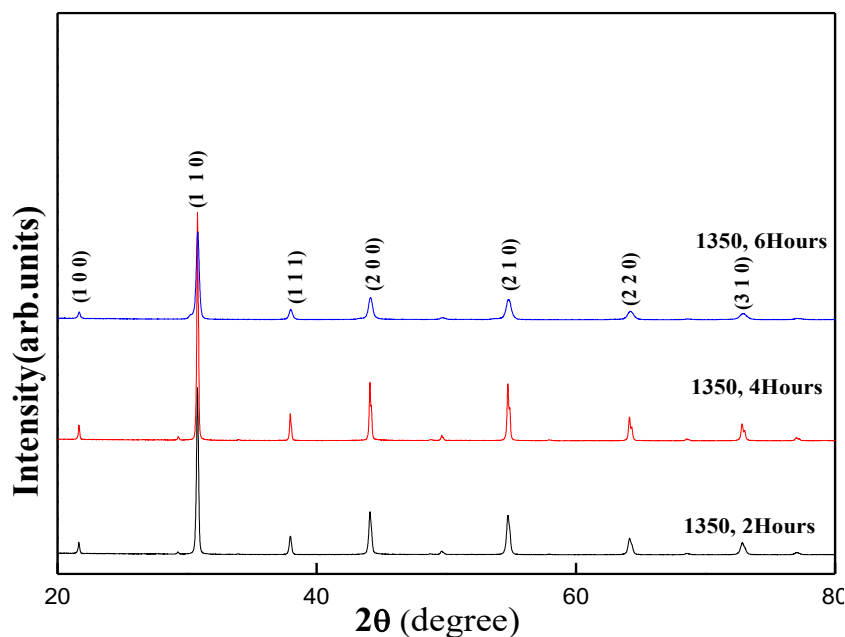


Figure 2. XRD profile of Nd doped BZT at various time periods

It is clear from the figure that the calcination period of 4 hour is suitable to get dominant single phase 'Nd' doped BZT compound by showing high intensity of the corresponding peak of around 31° . Hence forth further analysis on 'Nd' doped BZT compound was done at 1350 °C of calcined temperature and 4 hours duration of time.

To compare the crystallographic nature of undoped and 'Nd' doped BZT, performed the XRD analysis on both of them. The XRD spectra of pure BZT and 'Nd' doped BZT samples were shown in fig. 3. Pure BZT sample has shown the diffraction peaks at $2\theta = 31.2^\circ, 33.9^\circ, 37.9^\circ, 44.2^\circ, 54.6^\circ, 57.6^\circ, 64.1^\circ$ and 72.7° . In particular, by focusing on the peak observed at around 31° , the peak position

was shifted towards lower angles with the addition of 'Nd' into BZT. In-general there are some reports on shifting of the XRD peaks towards higher Bragg angles with addition of 'Nd' dopant into BaTiO_3 [14,15]. There were some other reports mentioned that the shift of diffraction peak towards lower Bragg angles with the addition of Zr into BaTiO_3 [16]. By analyzing the phenomenon on the shifting in the bragg's angle with addition of dopant, shifting in the 'Nd' doped BZT peak towards lower angles could be due to the fact that the either the atomic radii of Nd^{3+} (1.27 Å) is larger than that of Zr^{4+} (0.72 Å) and Ti^{4+} (0.605 Å) or the same of Ba^{2+} (1.61 Å) and Nd^{3+} are bit closer to each other.

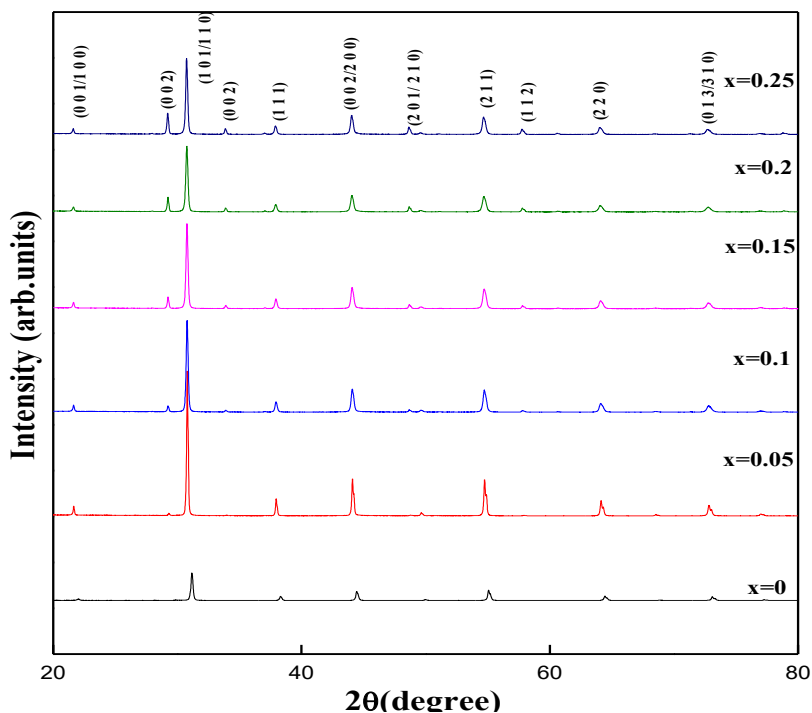


Figure 3. XRD spectra of Nd doped and un-doped BZT

The similar behavior was observed on further increment of 'Nd' doping percentage upto 0.15%, later on it got stabilized. In particular the high intensity peaks of BZT observed at 31.2° shifted to lower values of 30.80, 30.78 and 30.75° with the increase of 'Nd' doping levels from 0.05%, 0.1% and 0.15%, respectively. Aktas [9] reported that the shifting of XRD peaks towards lower 2θ values

could be due to the diffusion of high atomic radii BZ into low atomic radii BT lattice. In our study also the shift of dominant diffraction peak at around 31° shifted towards lower angles. It might be owing to the diffusion of high atomic radii Neodymium content (BN) might be diffused to low atomic radii Zr content (BZ).

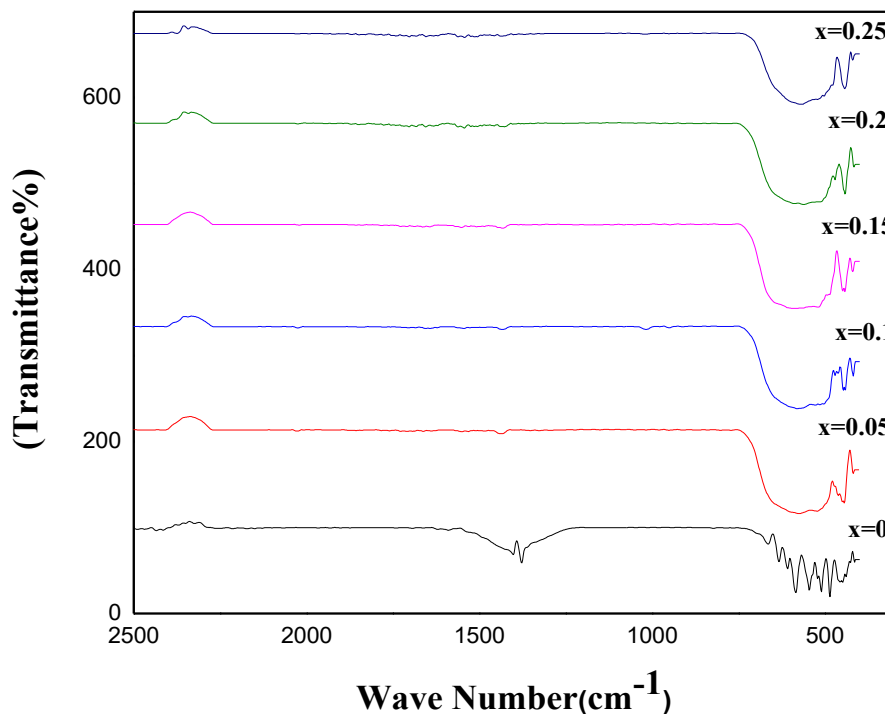


Figure 4. FTIR spectra of Nd doped and un-doped BZT

FTIR spectra

The FTIR spectra of the BaZrTiO₃ ceramics with various dopant concentration of Nd³⁺ were shown in Fig. 4. The addition of 'Nd' at various levels that, x: 0.0, 0.05, 0.1, 0.15, 0.20 and 0.25 %. FTIR spectra revealed that, by the addition of 'Nd' with 0.05% a significant broad band was observed in the range of 500 – 700 Cm⁻¹. This vibration was widened by shifting towards higher wavenumbers on increasing the 'Nd' percentage upto 0.15%. On further increment of 'Nd' percentage, leading to negative shift in the same vibrational broad band. The possible explanation for the positive and negative shifts of band was discussed below. The addition of Zr in Ti shows the absorption bands in the range of 540-580 cm⁻¹ were related to stretching vibrations of Ti-O-Ti and Zr-O-Zr [9, 12-17]. In our investigation also we observed the absorption bands at around 540 - 586 cm⁻¹ related to stretching vibrational modes of Ti-O and Zr-O. In particular, the addition of 'Nd' in the BZT, may increase the space between A and B sites, eventually broaden the absorption band, which was observed in pure BZT around the range of 540-586 cm⁻¹. The possible reason for this broadening of

this band could be owing to the presence of various radii ions, but also increase the host site vacancies [7].

The possible shift towards higher wave number range from 699-479 cm⁻¹ to 746-484 cm⁻¹ may be due to the identification of crystallographic structure in TiO_x, ZrO_x.

Surface morphology and atomic weight%

Figure 5 shows the SEM micrographs of 'Nd'-doped and undoped BZT ceramics calcined at 1350 °C. The SEM images showed that microstructure of the pure BZT has relatively larger grains when compare with 'Nd' doped BZT. In particular the average grain size of the undoped BZT was around 2 – 3 µm and the same was decreased abruptly to ~ 1.0 – 1.5 µm and 0.5 – 1 µm with the addition of 'Nd' concentration 0.05 and 0.1%, respectively. The possible explanation for this observation would be the higher order diffusion of 'Nd', resulting to improve the grain growth kinetics and densification of surface morphology and homogeneous grain distribution with smaller grains.

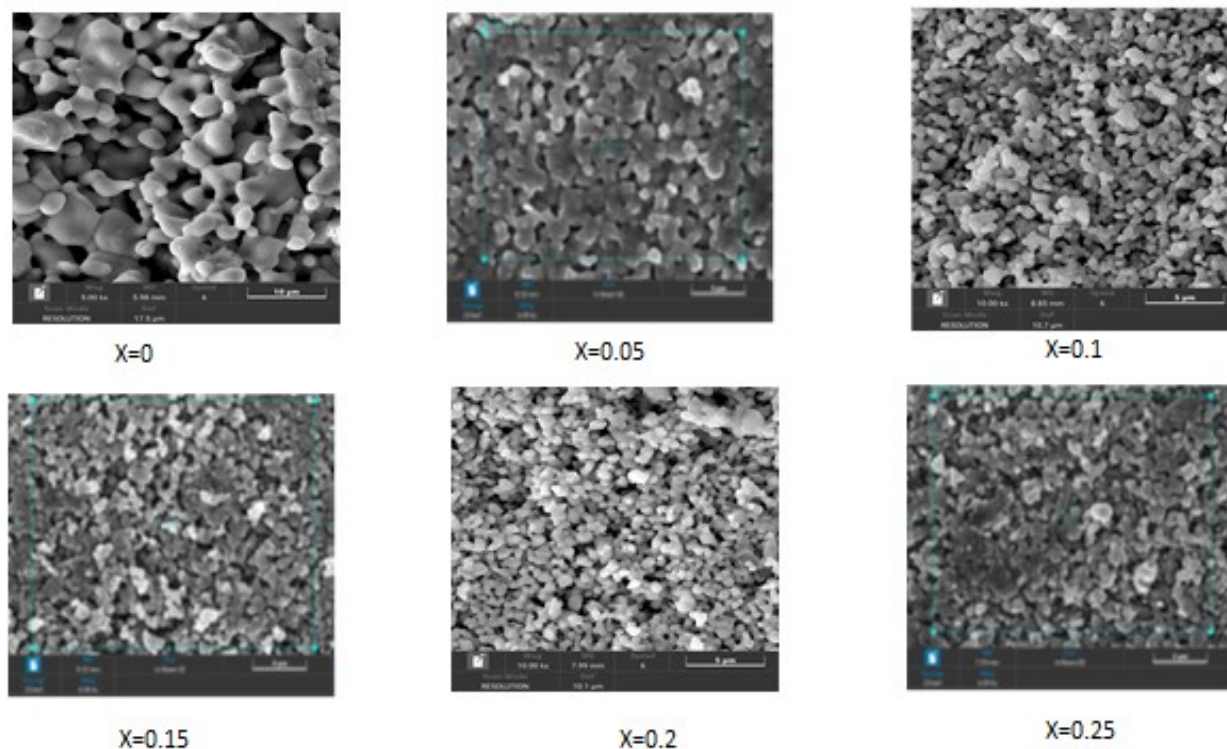


Figure 5. SEM images of Nd doped and un-doped BZT

Further increase in the 'Nd' concentration to there was a little increment in grain size, owing to lessening in the inter-diffusion kinetics between the particles, further increment in 'Nd' concentration improves the diffusion mechanism. With the increase of Nd³⁺ concentration in BZT, the atomic

% of 'Nd' varies from 1.87 to 5.63%, where as the corresponding weight percentage also increases from 4.88 to 14.50 by increasing the doping percentage from 0.05 to 0.25, respectively. On the other hand the atomic weight percentage of Ba content in BZT decreased accordingly.

4. CONCLUSIONS

The addition of 'Nd' in BZT significantly influenced the crystallographic and surface morphological properties on the basis of the individual elemental ionic radii. It was clearly confirmed by the XRD peaks by shifting the diffraction peak position towards lower Bragg's angles with the addition of 'Nd' content upto 0.15% and eventually reduction in the 2θ value further increment in the 'Nd' concentration. FTIR spectra also confirms the presence of Nd and increment in its percentage by shifting the vibration band towards higher wavenumbers. FESEM images strongly supported the above observed information.

5. REFERENCES

- [1] B.G. Naik, S.V.J.Chandra, S.Uthanna (2021) Influence of oxygen partial pressure on the structural, optical and electrical properties of magnetron sputtered $Zr_{0.7}Nb_{0.3}O_2$ films, *Appl. Phys. A*, 127, 127. doi: <https://doi.org/10.1007/s00339-021-05136-x>.
- [2] B. Vaishali, D. Tripathi (2024) Tuning low frequency dielectric properties of flexible ternary polymer blend film reinforced with bio- ionic liquid for the application in green electronics., *Zastita Materijala* 65 (1), 158. doi: <https://doi.org/10.62638/ZasMat1001>.
- [3] S.V.Jagadeesh Chandra, E. Fortunato, R. Martins, C.J. Choi (2012) Modulations in effective work function of platinum gate electrode in metal-oxide semiconductor devices, *Thin Solid Films*, 520, 4556-67. <https://doi.org/10.1016/j.tsf.2011.10.137>.
- [4] M. Reda, S.I. El-Dek, M. M. Arman (2022) Improvement of ferroelectric Properties via Zr doping in barium titanate nanoparticles, *J Mater Sci: Mater Electron.*, 33, 1675.
- [5] D.J. Shin, D.H. Lim, B.K. Koo, M.S. Kim, I.S. Kim, S.J. Jeong (2020) Porous sandwich structures based on $BaZrTiO_3$ - $BaCaTiO_3$ ceramics for piezoelectric energy harvesting, *Journal of Alloys and Compounds*, 831, 154792. doi: [10.1016/j.jallcom.2020.154792](https://doi.org/10.1016/j.jallcom.2020.154792)
- [6] X.G. Tang, K.H. Chew, H.L.W. Chan (2004) Diffuse phase transition and dielectric tunability of $Ba(Zr_yTi_{1-y})O_3$ relaxor ferroelectric ceramics, *Acta Mater.*, 52(17), 5177-5183. <https://doi.org/10.1016/j.actamat.2004.07.028>.
- [7] S.K. Ghosh, M. Ganguly, S.K. Rout, S. Chanda, T.P. Sinha (2014) Structural, optical and dielectric relaxor properties of neodymium doped cubic perovskite $(Ba(1-x)Nd_{2x/3})(Zr_{0.3}Ti_{0.7})O_3$, *Solid State Sci.*, 30, 68-77. doi: doi.org/10.1016/j.solidstatesciences.2014.02.007
- [8] R. Sagar, S. Madolappa, R. L. Raibagkar (2012) Electrical, dielectric and pyroelectric behavior of neodymium substituted barium zirconium titanate, *Solid State Sci.*, 14(2), 211-215. <https://doi.org/10.1016/j.solidstatesciences.2011.11.006>.
- [9] P.S. Aktaş (2020) Structural investigation of barium zirconium titanate $Ba(Zr_{0.5}Ti_{0.5})O_3$ particles synthesized by high energy ball milling process, *J. Chem. Sci.*, 132(1), 130. <https://doi.org/10.1007/s12039-020-01837-7>.
- [10] T. Maiti, R. Guo, A.S. Bhalla (2007) Enhanced electric field tunable dielectric properties of $BaZr_xTi_{(1-x)}O_3$ relaxor ferroelectrics, *Appl. Phys. Lett.*, 90, 182901-12. <https://doi.org/10.1063/1.2734922>.
- [11] S.B. Reddy, K.P. Rao, M.S.R. Rao (2009) Effect of La substitution on the "structural and dielectric properties of $BaZr_{0.1}Ti_{0.9}O_3$ ceramics, *J Alloys Comp.*, 481, 692-696. <https://doi.org/10.1016/j.jallcom.2009.03.075>.
- [12] S. Mittal, R. Laishram, K.C. Singh (2018) Improved electrical properties of lead-free neodymium doped $Ba_{0.85}Ca_{0.15}Zr_{0.1}Ti_{0.9}O_3$ piezoceramics, *Mater. Res. Bull.*, 105, 253-264. <https://doi.org/10.1016/j.materresbull.2018.04.036>.
- [13] S. Sasikumar, T.K. Thirumalaisamy, S.S. Kumar, S.A. Bahadur, D.Sivaganesh, I.B. Shameembanu (2020) Effect of Neodymium doping in $BaTiO_3$ ceramics on structural and Ferro electric properties, *J Mater. Sci. Mater. Electron.*, 31, 1535. <https://doi.org/10.1007/s10854-019-02670-6>.
- [14] N.A. Rejab, S. Sreekantan, K.A. Razak, Z.A. Ahmad (2011) Structural characteristics and dielectric properties of neodymium doped barium titanate, *J Mater Sci: Mater. Electron.*, 22, 167-176. <https://doi.org/10.1007/s10854-010-0108-9>.
- [15] Z. Wenxing, C. Lixin, W. Wenwen, S. Ge, L. Wei (2013) Effects of neodymium doping on dielectric and optical properties of $Ba_{(1-x)}Nd_xTi_{1.005}O_3$ ceramics, *Ceramics-Silikaty* 57(2), 146-155.
- [16] Z. Sun, Y. Pu, Z. Dong, Y. Hu, X. Liu, P. Wang (2014) Effect of Zr_{4b} content On the TC range and dielectric and ferroelectric properties of $BaZr_xTi_{(1-x)}O_3$ ceramics prepared by microwave sintering, *Ceramic. Intern.*, 40, 3589-3595. <https://doi.org/10.1016/j.ceramint.2013.09.069>
- [17] M. Reda, S.I. El-Dek, M.M. Arman (2022) Improvement of ferroelectric properties via Zr doping in barium titanate nanoparticles. *J Mater Sci: Mater Electron* 33, 16753-76. <https://doi.org/10.1007/s10854-022-08541-x>.

IZVOD

UTICAJ DOPANTA ND NA STRUKTURNA SVOJSTVA BARIJUM CIRKONIJUM TITANAT PEROVSKITA

Barijum cirkonijum titanat (BZT) nano kompozitni prah je pripremljen primenom metode reakcije u čvrstom stanju. Da bi se poboljšala strukturalna svojstva BZT, neodimijum je dopiran na različitim nivoima koncentracije. Za analizu termičke stabilnosti neodimijumom (Nd) dopiranog BZT-a, proces kalcinacije je izveden na različitim temperaturama u opsegu od 1150, 1200, 1250, 1300 i 1350 °C tokom 4 sata. XRD spektri uzorka kalcinisanog na 1350 °C tokom 4 sata dali su značajne pikove u poređenju sa drugim temperaturama. Dalje, primećeno je da je kristalografska priroda uzorka poboljšana povećanjem procenta Nd u BZT. FTIR spektri potvrđuju prisustvo BZT i na kraju odgovarajući pomak u trakama uz dodavanje Nd. Osim toga, povećanjem procenta Nd u BZT došlo je do pomeranja položaja širokog pojasa ka višem opsegu talasnih brojeva od [699-479]cm⁻¹ do [746-484]cm⁻¹, na kraju kristalografske prirode TiO₂. Jedinjenja ZrO₂ i Nd₂O₃ potvrđena su pomeranjem vibracionog opsega ka nižoj talasnoj dužini u opsegu od [746-484] cm⁻¹ do [735-480] cm⁻¹. Elektronski mikroskopski snimci skeniranja emisije polja ilustruju da su uzorci BZT dopiranog 'Nd' bili relativno porozni u poređenju sa nedopiranim BZT.

Ključne reči: barijum cirkonijum titanat, neodim, kuglično mlevenje, kristalografska struktura, morfologija površine.

Naučni rad

Rad primljen: 12.06.2024.

Rad korigovan: 19.09.2024.

Rad prihvaćen: 10.10.2024.

CH. Swathi:	https://orcid.org/0000-0003-0365-5339
S.V. Jagadeesh Chandra:	https://orcid.org/0000-0001-6418-9066
Y.Srinivasa Rao:	https://orcid.org/0000-0003-4876-3093
D.V.Rama Koti Reddy:	https://orcid.org/0000-0002-8829-5282